

学位論文

**Differential reactivation of fetal/neonatal genes in mouse
liver tumors induced in cirrhotic and noncirrhotic conditions**

マウス肝腫瘍における胎児・新生児期遺伝子の再活性化：
肝硬変・非肝硬変モデルの比較検討

旭川医科大学大学院医学系研究科博士課程医学専攻

陳 錫

(山本雅大、藤井清永、永濱康晴、大塩貴子、
辛冰、岡田陽子、古川博之、西川祐司)

1 **Differential reactivation of fetal/neonatal genes in mouse liver tumors induced in**
2 **cirrhotic and noncirrhotic conditions**

3 Xi Chen,¹ Masahiro Yamamoto,¹ Kiyonaga Fujii,¹ Yasuharu Nagahama,¹ Takako Ooshio,¹ Bing Xin,¹
4 Yoko Okada,¹ Hiroyuki Furukawa,² and Yuji Nishikawa¹

5
6 ¹Division of Tumor Pathology, Department of Pathology, Asahikawa Medical University, Asahikawa,
7 Hokkaido 078-8510, Japan

8 ²Division of Gastroenterological and General Surgery, Department of Surgery, Asahikawa Medical
9 University, Asahikawa, Hokkaido 078-8510, Japan

10
11 **Corresponding author:** Yuji Nishikawa, Division of Tumor Pathology, Department of Pathology,
12 Asahikawa Medical University, Higashi 2-1-1-1, Midorigaoka, Asahikawa, Hokkaido 078-8510,
13 Japan. Tel: +81-166-68-2370; Fax: +81-166-68-2379. E-mail: nishikwa@asahikawa-med.ac.jp

14 **Conflicts of interest:** No conflicts of interest exist in this study.

15 **Grant support:** This work was supported by grants from the Ministry of Education, Culture, Sports,
16 Science, and Technology of Japan (#18590362, #21590426, and #24390092) to Yuji Nishikawa.

17 **Key words:** hepatocellular carcinoma, liver cirrhosis, mRNA expression, insulin-like growth factor 2,
18 trefoil factor 3

19 **Word count:** 3552; **Number of figures:** 8; **Number of tables:** 2

1 **Summary**

2 Hepatocellular carcinoma develops in either chronically injured or seemingly intact livers. To
3 explore the tumorigenic mechanisms underlying these different conditions, we compared the mRNA
4 expression profiles of mouse hepatocellular tumors induced by the repeated injection of CCl₄ or a
5 single diethylnitrosamine (DEN) injection using a cDNA microarray. We identified tumor-associated
6 genes that were expressed differentially in the cirrhotic CCl₄ model (*H19*, *Igf2*, *Cbr3*, and *Krt20*) and
7 the noncirrhotic DEN model (*Tff3*, *Akr1c18*, *Gpc3*, *Afp*, and *Abcd2*) as well as genes that were
8 expressed comparably in both models (*Ly6d*, *Slpi*, *Spink3*, *Scd2*, and *Cpe*). The levels and patterns of
9 mRNA expression of these genes were validated by RT-qPCR analyses. Most of these genes were
10 highly expressed in mouse livers during the fetal/neonatal periods. We also examined the mRNA
11 expression of these genes in mouse tumors induced by thioacetamide, another cirrhotic inducer, and
12 those that developed spontaneously in noncirrhotic livers and found that they shared a similar
13 expression profile as that observed in CCl₄-induced and DEN-induced tumors, respectively. There
14 was a close relationship between the expression levels of *Igf2* and *H19* mRNA, which were activated
15 in the cirrhotic models. Our results show that mouse liver tumors reactivate fetal/neonatal genes,
16 some of which are specific to cirrhotic or noncirrhotic modes of pathogenesis.

17

1 **Introduction**

2 Various risk factors for hepatocellular carcinoma (HCC) exist, including infection with
3 hepatitis B and C viruses, alcoholic and nonalcoholic fatty liver disease, and several hereditary
4 metabolic diseases.⁽¹⁾ However, chronic liver injury, typically cirrhosis, is the most important and
5 common setting for the development of HCC. Although recent studies have revealed critical roles of
6 the interleukin-6/JAK/STAT pathway and the NF- κ B pathway and the possible involvement of the
7 inflammasome, the exact mechanisms underlying the development of HCC in chronic liver disease
8 remain obscure.⁽²⁾ Furthermore, a small fraction of HCC has been known to occur in patients with a
9 seemingly intact liver. Such noncirrhotic HCC may share several characteristics with hepatocellular
10 adenoma,⁽³⁾ which has been shown to undergo malignant transformation with an overall frequency of
11 4.2%.⁽⁴⁾ There might be different tumorigenic mechanisms between tumors associated with chronic
12 injury or cirrhosis and those that develop in seemingly intact livers.

13 A variety of mouse models of hepatocarcinogenesis have been used to elucidate the
14 mechanisms underlying the development of HCC. The most widely used is the diethylnitrosamine
15 (DEN)-induced model,⁽⁵⁾ in which hepatocellular adenoma and HCC develop in an intact,
16 noncirrhotic liver. Several liver tumor-prone transgenic mouse lines have also been generated by the
17 introduction of HBsAg and HBx,⁽⁶⁾ SV40 large T antigen, a secretable form of EGF,⁽⁷⁾ or oncogenes
18 such as E2F-1, c-Myc, and transforming growth factor- α .⁽⁸⁾ In these models, liver tumors also
19 developed in noncirrhotic livers; thus, the results that were obtained need to be interpreted cautiously
20 when they are extrapolated for understanding the pathogenesis of human HCC that develops in

1 fibrotic or cirrhotic backgrounds. Conversely, long-standing centrilobular injury inflicted by the
2 chronic administration of CCl₄ or thioacetamide (TAA) in adult mice can induce liver tumors in a
3 fully established cirrhotic background.^(9, 10)

4 In the present study, to gain insights into the tumorigenic mechanisms in cirrhotic and
5 noncirrhotic conditions, we compared the mRNA expression profiles of mouse liver tumors induced
6 by the repeated injection of CCl₄ (cirrhotic protocol) or a single DEN injection when the mice were 2
7 weeks old (noncirrhotic protocol) using a cDNA microarray and RT-qPCR. We identified several
8 genes whose mRNA expression was increased predominantly in either CCl₄-induced or
9 DEN-induced liver tumors as well as genes that were increased comparably in both. We further
10 examined the mRNA expression of the identified genes, most of which were also highly expressed in
11 the fetal/neonatal liver, in other mouse liver tumors induced under cirrhotic and noncirrhotic
12 conditions.

14 **Materials and Methods**

15 **Animals**

16 C3H/HeNCr1Cr1j (C3H) and C57BL/6J (C57) mice were purchased from Charles River
17 Laboratories Japan (Yokohama, Japan). C3H × C57 F1 offspring were generated by breeding male
18 C3H and female C57 mice. The mice were euthanized under deep anesthesia, and the livers were
19 removed for further examination. The protocols used for animal experimentation were approved by
20 the Animal Research Committee, Asahikawa Medical University, and all animal experiments adhered

1 to the criteria outlined in the Guide for the Care and Use of Laboratory Animals prepared by the
2 National Academy of Sciences (8th Ed., 2011).

4 **Mouse liver tumor models**

5 Male C3H × C57 F1 or C57 mice (8- to 10-week-old) were treated with CCl₄ (Kanto
6 Chemical, Tokyo, Japan) 3 times per week (1 ml/kg, s.c.; 1:5 dilution in olive oil) for 24 weeks to
7 induce liver cirrhosis and subsequent tumor formation. Male C3H × C57 F1 mice were also treated
8 with thioacetamide (TAA; Sigma-Aldrich, St. Louis, MO) administration (0.03% in drinking water)
9 for 30 weeks to generate another cirrhotic model of liver tumors.

10 To induce liver tumors in a noncirrhotic background, C3H × C57 F1 mice were treated with
11 a necrotizing dose of DEN (5 mg/kg, i.p.) at 2 weeks after birth and euthanized after 44 weeks. As
12 another noncirrhotic model, liver tumors that had spontaneously developed in C3H mice aged 13-15
13 months were analyzed.⁽¹¹⁾

15 **cdNA microarray analysis**

16 Total RNA was prepared from snap frozen liver tissues using the RNeasy Mini Kit (Qiagen).
17 Samples of CCl₄-induced liver tumors (a mixture of 5 independent large tumors), DEN-induced liver
18 tumors (a mixture of 5 independent large tumors), CCl₄-induced cirrhotic liver tissues (non-tumorous
19 tissues of the livers harboring tumors) (a mixture of 5 tissues from 5 mice), and control liver tissue
20 (olive oil-treated; a mixture of 2 tissues from 2 mice) were analyzed and compared by one-color

1 microarrays (3D-Gene Microarray, TORAY, Tokyo, Japan). After background subtraction, the raw
2 microarray data were normalized using a standard global normalization technique, and the signal
3 intensities were calculated as the fold changes of expression values. The data of differentially
4 expressed genes that were significantly changed (> 4 -fold, compared with control) were subjected to
5 Z-score transformation and loaded in a centroid-linkage hierarchical clustering assay using a Pearson
6 correlation (uncentered) similarity metric with Cluster 3.0. Then, the Java TreeView software
7 (<http://jtreeview.sourceforge.net/>) was applied to reveal the hierarchical gene groups among the four
8 samples. The Z-score was cropped to -1.5 to +1.5 when generating a two-color heat map.

9

10 **Quantitative reverse transcriptase-polymerase chain reaction (RT-qPCR)**

11 Total RNA were extracted from frozen liver tissues and subjected to quantitative real-time
12 RT-PCR (RT-qPCR) analyses. RT-qPCR was performed using the $\Delta\Delta C_t$ method with the FastStart
13 Universal SYBR Green Master Mix (Roche Diagnostics, Mannheim, Germany). Each reaction was
14 conducted in duplicate, and the mRNA levels were normalized to glyceraldehyde-3-phosphate
15 dehydrogenase (*Gapdh*). The sequences of the specific primers are listed in Table S1.
16 Two-dimensional hierarchal clustering of tumor-associated genes was performed using
17 Z-score-normalized data. The Z-score was cropped to -2.0 to +2.0 when generating a two-color heat
18 map.

19

20

1 **Microscopic examination, immunohistochemistry, and *in situ* hybridization**

2 The livers were fixed in phosphate-buffered 10% formalin for 24 hours, and paraffin
3 sections were then prepared. Immunohistochemical staining was performed with the EnVision/HRP
4 system (DAKO, Carpinteria, CA) on deparaffinized sections treated with Target Retrieval Solution
5 (DAKO). The antibodies used were as follows: anti-IGF2 (ab9574, Abcam, Cambridge, UK),
6 anti- α -fetoprotein (AFP) (14550-1-AP, Proteintech Group, Chicago, IL; for mouse tissues), anti-AFP
7 (A0008, DAKO, for human tissues), and anti-TFF3 (Abbiotec, San Diego, CA).
8 3,3'-diaminobenzidine tetrahydrochloride (Vector Laboratories, Burlingame, CA) was used for signal
9 detection. For the detection of the TFF3 peptide, we applied signal amplification using the TSA Plus
10 DIG Kit (PerkinElmer, Waltham, MA). *In situ* hybridization for non-coding *H19* mRNA was
11 performed on deparaffinized sections using the mouse H19 QuantiGene ViewRNA Probe Set
12 (VB6-16706, Affymetrix, Santa Clara, CA) and the QuantiGene ViewRNA ISH Tissue Assay Kit
13 (Affymetrix).

14

15 **Human liver samples**

16 The retrospective analysis of surgical specimens was approved by the internal review board
17 of Asahikawa Medical University. A total of 33 HCC samples from patients who had curative
18 hepatectomy and 5 intact liver tissues surrounding the resected cavernous hemangiomas were
19 collected. Among the HCC samples, 9 cases were devoid of any detectable fibrosis or inflammation
20 in the non-tumorous liver parenchyma, whereas the rest showed various degrees of liver fibrosis

1 (fibrous expansion of the portal tract, bridging fibrosis, and cirrhosis).

2

3 **Statistical analysis**

4 Unpaired two-tailed *t*-tests or one-way analysis of variance were used to compare
5 differences in gene expression. The correlation between Ki-67 staining and the mRNA levels of
6 genes was assessed by Spearman's correlation coefficients. Fisher's exact test was used to evaluate
7 the differences in expression of various proteins in HCC samples between the groups with and
8 without liver fibrosis.

9

10 **Results**

11 **cDNA microarray analyses of differentially expressed genes in CCl₄-induced and DEN-induced** 12 **mouse liver tumors**

13 Following repeated injections of CCl₄, numerous relatively small tumors appeared in the
14 markedly fibrotic and cirrhotic liver parenchyma, whereas in the DEN model, multiple large tumors
15 developed in the noncirrhotic background (Fig. 1a). Histologically, both CCl₄- and DEN-induced
16 tumors were hepatocyte tumors, with features of hepatocellular adenoma and well-differentiated
17 HCC (Fig. 1b). The surrounding non-tumorous liver tissues were cirrhotic in the CCl₄ model but
18 were almost normal and noncirrhotic in the DEN model, as revealed by sirius red staining (Fig. 1b).
19 The cDNA microarray analysis identified 1,028 differentially expressed genes in the intact liver
20 tissues (control), CCl₄-induced cirrhotic tissues (non-tumor, NT) (CCl₄-NT), CCl₄-induced tumors

1 (CCl₄-T), and DEN-induced tumors (DEN-T) across genetic clusters A-D (Fig. 1c). Several genes,
2 such as *S100g*, *Cyp4a14*, and *Mmp7*, were selectively activated in cirrhotic tissues (CCl₄-NT), while
3 the expression of others, such as *Fabp6* and *Plat*, was increased in both CCl₄-NT and CCl₄-induced
4 tumors (CCl₄-T) (Table S2). We focused on the tumor-associated genes that were highly expressed in
5 either CCl₄- or DEN-induced tumors (Tables 1 and 2).

6 7 **Validation of mRNA expression profiles by RT-qPCR and *in situ* detection of IGF2, *H19* mRNA, 8 **TFF3, and AFP in tumors****

9 The levels and patterns of mRNA expression of the identified genes were validated by
10 RT-qPCR analyses. The mRNA expression of *H19*, *Igf2*, *Cbr3*, and *Krt20* was predominantly
11 increased in CCl₄-induced tumors (more than 4-fold that observed in DEN-induced tumors;
12 “CCl₄-associated”); that of *Tff3*, *Akr1c18*, *Gpc3*, *Afp*, and *Abcd2* was predominantly increased in
13 DEN-induced tumors (more than 4-fold over that in CCl₄-induced tumors; “DEN-associated”); and
14 that of *Ly6d*, *Slpi*, *Spink 3*, *Scd2*, and *Cpe* was increased at comparable levels in CCl₄- and
15 DEN-induced tumors (“Common”) (Fig. 2a). The changes in mRNA expression observed in the
16 remaining genes (*Cib3*, *Top2a*, *Cdkn2b*, *Pnpla5*, and *Tspan8*) in the tumors were not statistically
17 significant (Fig. S1).

18 Among the changes in mRNA expression associated with CCl₄-induced tumors, an increase
19 in *Igf2* and *H19* mRNA was the most specific and was found in approximately half of the tumors (see
20 Fig. 6). In addition, the magnitude of the induction of *Tff3* mRNA, especially in DEN-tumors, was

1 very impressive. To confirm the protein expression of IGF2 and TFF3 and the mRNA expression of
2 *H19* in liver tumors, we performed immunohistochemistry for IGF2 and TFF3 and *in situ*
3 hybridization for *H19*. The expression of α -fetoprotein (AFP), a prototype oncofetal marker for HCC,
4 was also examined. Although all of these were negative in adult liver tissues, IGF2 was positive in
5 approximately half of CCl₄-induced tumors but completely negative in DEN-induced tumors (Fig.
6 2b). *H19* mRNA was strongly expressed in some of CCl₄-induced tumors (Fig. 2b). DEN-induced
7 tumors also expressed *H19* mRNA, but its levels were generally low (Fig. 2b). Although TFF3 was
8 detected in both types of tumors, DEN-induced tumors tended to show stronger staining (Fig. 2b).
9 AFP was strongly positive in DEN-induced tumors, whereas CCl₄-induced tumors were negative or
10 contained scattered positive cells (Fig. 2b).

11

12 **Relationship between the proliferative activity of tumor cells and the mRNA expression levels** 13 **of the tumor-associated genes**

14 We next examined whether the mRNA expression of the tumor-associated genes correlated
15 with tumor cell proliferation, as estimated by Ki-67 immunohistochemistry. In the CCl₄ model, the
16 expression levels of *Cbr3* and *Tff3* were correlated with the proliferative activity of the tumor cells
17 (Fig. 3). Although *Igf2* encodes insulin-like growth factor 2 (IGF2), which has been shown to play
18 important roles in cell growth, *Igf2* mRNA expression was not significantly correlated with tumor
19 cell proliferation, similar to other genes (Fig. 3, Fig. S2). In the DEN model, the expression of none
20 of the genes analyzed was related to the proliferative activity of the tumor cells (Fig. 3, Fig. S2).

1
2
3
4
5
6
7
8
9
10
11
12
13
14
15
16
17
18
19
20

Fetal or neonatal expression of the tumor-associated genes

Because the identified tumor-associated genes included well-known oncofetal genes, such as *Igf2*, *H19*, *Gpc3*, and *Afp*, we examined their mRNA expression during fetal and neonatal periods. Our results clearly showed that all of these genes, with the exceptions of *Cbr3* and *Cpe*, were highly expressed in either the fetal or neonatal periods (Fig. 4a), indicating that the differential activation of fetal/neonatal gene expression occurs in CCl₄- and DEN-induced liver tumors. As expected, the protein expression of IGF2 and TFF3 and the mRNA expression of *H19* were detected in hepatoblasts/hepatocytes during the fetal or neonatal period (Fig. 4b).

Comparison with other cirrhotic and noncirrhotic liver tumor models

Next, we examined whether similar differential activation could also be observed in other liver tumor models. TAA-induced selective centrilobular injuries and chronic TAA administration resulted in multiple liver tumors (hepatocellular adenoma or well differentiated HCC), which were associated with marked cirrhosis in the surrounding liver (Fig. 5a). In TAA-induced tumors, there were increases in the expression of *Igf2* mRNA and *Krt20* mRNA, with a tendency for increased mRNA expression of *H19* and *Igf2bp3* (Fig. 5b). In contrast, the mRNA expression of *Akr1c18*, *Gpc3*, and *Afp*, which was highly characteristic of DEN-induced tumors, was not observed in TAA-induced tumors, although there was an increase in *Abcd2* mRNA (Fig. 5b). In spontaneously formed liver tumors (well to moderately differentiated HCC) in the intact livers of aged C3H mice,

1 there was no increase in the mRNA expression of the genes that were selectively increased in
2 CCl₄-induced tumors, but the mRNA expression of *Tff3*, *Akr1c18*, *Afp*, and *Abcd2* was significantly
3 increased (Fig. 5b). The mRNA expression of all the “common” genes was increased in
4 TAA-induced tumors, whereas that of *Spink3*, *Scd2*, and *Cpe* was lacking in the spontaneously
5 formed tumors (Fig. 5b).

6 7 **Two-dimensional hierarchical cluster analysis of the tumor-associated genes in the cirrhotic** 8 **and noncirrhotic models**

9 The mRNA expression data of the 15 tumor-associated genes in the 4 different liver tumor
10 models (CCl₄-induced, DEN-induced, TAA-induced, spontaneous) were subjected to unsupervised
11 two-dimensional hierarchical cluster analysis (Fig. 6). Interestingly, the mRNA expression profiles of
12 the 15 genes almost clearly segregated control liver tissues, cirrhotic tissues, and tumors that had
13 developed in the cirrhotic and noncirrhotic backgrounds. Furthermore, there were several clusters of
14 between 2 and 4 transcripts, which characterized tumors that had developed in the cirrhotic
15 background (*H19*, *Igf2*, and *Igf2bp3*), in the noncirrhotic background (*Tff3*, *Akr1c18*, *Abcd2*, and
16 *Gpc3*), and in either background (*Scd2* and *Slpi*; *Cpe* and *Ly6d*).

17 18 **Selective activation of *IGF2* and its related genes in CCl₄- or TAA-induced tumors**

19 There was a significant positive correlation between the mRNA expression levels of *Igf2* and *H19*
20 (Fig. 7a), which are known to be adjacently located in the genome and are regulated through

1 reciprocal imprinting and a common enhancer.^(12, 13) The mRNA expression of *Igf2bp3*, whose
2 product is functionally correlated with *Igf2* mRNA and *H19* mRNA,⁽¹⁴⁾ was also increased in
3 CCl₄-induced tumors (Fig. 2). The expression of *Igf2bp3* mRNA was significantly higher in tumors
4 with substantial levels of *Igf2* mRNA expression ($Igf2/Gapdh \geq 0.01$) compared with those that
5 exhibited very low or no *Igf2* mRNA expression ($Igf2/Gapdh < 0.01$) (Fig. 7b). Similar findings were
6 obtained with TAA-induced tumors (Fig. 7a, b).

7

8 **Expression of IGF2, TFF3, and AFP in human HCC with or without liver fibrosis**

9 The above experiments demonstrated that IGF2 expression showed significant
10 discrimination ability for mouse liver tumors developed in cirrhotic and noncirrhotic backgrounds.
11 We examined IGF2 expression in human HCC developed with seemingly intact (nonfibrotic) livers
12 or fibrotic livers. Immunohistochemically, tumor cells stained positive for either IGF2, TFF3, or AFP
13 were found in several HCC cases, while these were negative in the surrounding liver parenchyma
14 (Fig. 8a). Clusters of IGF2-positive tumor cells were present in 11.1% and 54.2% of HCC developed
15 with nonfibrotic livers (n = 9) and those developed with fibrotic livers (n = 24), respectively (Fig. 8b).
16 This difference was statistically significant (p = 0.0466, Fisher's exact test). In contrast, there were
17 no significant differences in the expression of TFF3 and AFP in HCC developed under these
18 different conditions (Fig. 8b).

19

20

1 Discussion

2 We identified genes whose mRNA expression was increased in mouse liver tumors induced
3 in cirrhotic and noncirrhotic conditions. Based on gene expression clustering of these genes, we
4 could distinguish tumors arising in the two different backgrounds, indicating the presence of genes
5 that are differentially expressed during the tumorigenic course. Interestingly, most of the
6 tumor-associated genes were also activated in the fetal/neonatal periods. The activation of these
7 genes, including well established oncofetal genes (e.g., *Afp*, *Igf2*, *H19*, and *Gpc3*),⁽¹⁵⁻¹⁷⁾ occurred in
8 the late fetal period (E16.5) and persisted during the postnatal period. This finding indicates that the
9 mRNA expression of these genes in the liver tumors might not reflect the simple dedifferentiation of
10 transformed hepatocytes into immature hepatoblasts. Although the significance of the reactivation of
11 fetal/neonatal genes in mouse liver tumors is unclear, our study demonstrates that transformed
12 hepatocytes might utilize the cellular system that is active during the fetal/neonatal periods, when the
13 most robust physiological proliferation of hepatocytes occur.⁽¹⁸⁾

14 *Tff3* mRNA and its product, an intestinal polypeptide, trefoil factor 3 (TFF3), were highly
15 expressed in mouse liver tumors, particularly in those induced by DEN in C3H × C57 F1 and those
16 that developed spontaneously in C3H mice. TFF3 polypeptide was also detected in human HCC
17 arising in either fibrotic or nonfibrotic liver. It has been reported that *Tff3* mRNA expression is
18 increased in spontaneous liver tumors in tumor-prone PWK mice and those that develop in SV40 T
19 antigen transgenic mice, as well as in human HCC.⁽¹⁹⁾ Marked increases in *Tff3* mRNA have also
20 been found in liver tumors that developed in *HBx* transgenic mice⁽²⁰⁾ and those that developed in

1 secretable EGF-expressing transgenic mice.⁽⁷⁾ The expression of *Tff3* mRNA is governed by several
2 transcription factors, including hepatocyte nuclear factor 3 and NF-κB, and by DNA methylation of
3 its promoter region. Specifically, promoter hypomethylation has been found in mouse liver tumors
4 and human HCC.⁽¹⁹⁾ Although TFF3 is highly expressed in goblet cells in the intestinal mucosa and
5 has been suggested to be important in the processes of mucosal repair,⁽²¹⁾ its role in
6 hepatocarcinogenesis is currently obscure. However, *Tff3* mRNA or TFF3 polypeptide may serve as
7 useful biomarkers due to their high specificity to liver tumors.

8 Our study demonstrated that *Igf2* and its related genes, *H19* and *Igf2bp3*, were selectively
9 activated in approximately half of the mouse liver tumors induced under cirrhotic, but not
10 noncirrhotic conditions. The expression of *Igf2bp3* mRNA was significantly higher in the
11 *Igf2*-expressing tumors induced by CCl₄, suggesting their functional correlation. *Igf2* and *H19*, which
12 is located immediately downstream of *Igf2*, are reciprocally imprinted through the hypomethylation
13 and methylation of the differentially methylated region on the maternal allele and paternal allele,
14 respectively, and their expression is dependent on the two endoderm-specific enhancers that lie 3' of
15 *H19*.⁽¹²⁾ Although we do not know whether the loss of imprinting or altered methylation states of this
16 gene cluster might contribute to their activation, a highly significant correlation between the *Igf2*
17 mRNA and *H19* mRNA levels in the tumors suggests that their transcriptional activation is mediated
18 by common enhancers.⁽¹³⁾ Increased mRNA expression of *IGF2* and *H19*, as well as a significant
19 correlation of their mRNA expression levels, have been demonstrated in human HCC.⁽²²⁻²⁵⁾ However,
20 following a partial hepatectomy in rodents, whereas *H19* mRNA is markedly induced, *Igf2* mRNA

1 expression is not activated,⁽²⁶⁾ indicating a striking contrast between nontransformed and transformed
2 hepatocytes.

3 Our analysis of human liver samples showed the lower frequency of IGF2 positivity in
4 tumor cells in the cases of HCC arising in almost intact liver, compared with those with various
5 degrees of fibrosis. Interestingly, in an attempt of transcriptional classification of human HCC into 6
6 subgroups, an identified subgroup (G1) was characterized by the reactivation of *IGF2* gene
7 expression, as well as the association with HBV infection.⁽²⁵⁾ While further confirmation is needed in
8 view of the small number of cases analyzed, our data suggest the possible involvement of the IGF2
9 signaling in human hepatocarcinogenesis that is associated with chronic liver injury and fibrosis.

10 Although the exact mechanisms of HCC development in chronically injured and fibrotic
11 liver are not clear, it is probable that the continued stimuli for hepatocyte regeneration following
12 liver injury may play important roles in this process.⁽²⁷⁾ Repeated hepatocyte injury promotes hepatic
13 tumorigenesis in HCV transgenic mice,⁽²⁸⁾ possibly through excessive EGFR and/or c-Met signaling
14 activities.⁽²⁷⁾ While our study elucidated the close association between the activation of *Igf2* gene
15 expression and the cirrhotic hepatocarcinogenesis, reactivation of *Igf2* gene expression in liver
16 tumors has been demonstrated in the absence of liver injury in various experimental models with
17 enhanced hepatocyte proliferation in whole livers, such as *HBx* and *SV40 T Ag* transgenic mice.^{(20, 29,}
18 ³⁰⁾ In *SV40 T Ag* transgenic mice, as well as in HBV presurface gene (*preS1* and *preS2*) transgenic
19 mice, in which benign and malignant hepatocytic nodules appear following perpetual hepatocyte
20 apoptosis and regeneration, IGF2 reactivation has been found to be associated with late progression

1 steps toward HCC.⁽³⁰⁾ Furthermore, in secretable EGF-expressing transgenic mice, there is a switch
2 from the initial EGF-dependent state to an EGF-independent, IGF2-dependent state during
3 tumorigenesis.⁽³¹⁾ Thus, the reactivation of *Igf2* gene expression in liver tumors might reflect the
4 presence of continuous hepatocyte proliferation in the liver parenchyma, in which preneoplastic or
5 neoplastic hepatocytes are eventually generated. In contrast, in the noncirrhotic (DEN-induced and
6 spontaneous) models, liver tumor formation may be mainly dependent on induced or spontaneous
7 stochastic somatic mutations, which render some of the altered hepatocytes more proliferative than
8 the surrounding intact hepatocytes. Because epigenetic alterations, including losses and gains of
9 DNA methylation, have been increasingly recognized to occur during carcinogenesis,^(32, 33) we
10 speculate that epigenetically regulated genes might serve as signatures of distinctive modes of liver
11 tumor formation.

12 In conclusion, by studying transcriptome characteristics, we have shown that the mouse
13 liver tumors induced in cirrhotic and noncirrhotic conditions differentially reactivate various
14 fetal/neonatal genes. In particular, our data raise the possibility that the IGF2 axis could be
15 selectively activated in liver tumors induced by excessive proliferative stimuli following chronic
16 liver injury.

17

18 **Acknowledgements**

19 We would like to thank Mr. Yoshiyasu Satake for animal care and Ms. Ema Yamatomi and Ms.
20 Hiroko Chiba for secretarial assistance. We are also grateful to the staff of the Department of

1 Pathology, Asahikawa Medical University Hospital for generous help.

2

3 **Disclosure Statement**

4 The authors have no conflict of interest to declare.

5

1 **References**

- 2 1. El-Serag HB. Hepatocellular carcinoma. *N Engl J Med* 2011;**365**: 1118-1127.
- 3 2. Ramakrishna G, Rastogi A, Trehanpati N, Sen B, Khosla R, Sarin SK. From cirrhosis to
4 hepatocellular carcinoma: new molecular insights on inflammation and cellular senescence. *Liver*
5 *Cancer* 2013;**2**: 367-383.
- 6 3. Liu TC, Vachharajani N, Chapman WC, Brunt EM. Noncirrhotic hepatocellular carcinoma:
7 derivation from hepatocellular adenoma? Clinicopathologic analysis. *Mod Pathol* 2014;**27**: 420-432.
- 8 4. Stoot JH, Coelen RJ, De Jong MC, Dejong CH. Malignant transformation of hepatocellular
9 adenomas into hepatocellular carcinomas: a systematic review including more than 1600 adenoma
10 cases. *HPB (Oxford)* 2010;**12**: 509-522.
- 11 5. Vesselinovitch SD. Infant mouse as a sensitive bioassay system for carcinogenicity of
12 N-nitroso compounds. *IARC Sci Publ* 1980: 645-655.
- 13 6. Wang Y, Cui F, Lv Y, Li C, Xu X, Deng C, Wang D, Sun Y, Hu G, Lang Z, Huang C, Yang
14 X. HBsAg and HBx knocked into the p21 locus causes hepatocellular carcinoma in mice.
15 *Hepatology* 2004;**39**: 318-324.
- 16 7. Borlak J, Meier T, Halter R, Spanel R, Spanel-Borowski K. Epidermal growth
17 factor-induced hepatocellular carcinoma: gene expression profiles in precursor lesions, early stage
18 and solitary tumours. *Oncogene* 2005;**24**: 1809-1819.
- 19 8. Calvisi DF, Factor VM, Ladu S, Conner EA, Thorgeirsson SS. Disruption of beta-catenin
20 pathway or genomic instability define two distinct categories of liver cancer in transgenic mice.

- 1 *Gastroenterology* 2004;**126**: 1374-1386.
- 2 9. Edwards JE. Hepatomas in mice induced with carbon tetrachloride. *J Natl Cancer Inst*
3 1941;**2**: 197-199.
- 4 10. Gothoskar SV, Talwalkar GV, Bhide SV. Tumorigenic effect of thioacetamide in Swiss
5 strain mice. *Br J Cancer* 1970;**24**: 498-503.
- 6 11. Andervont HB. Studies on the occurrence of spontaneous hepatomas in mice of strains C3H
7 and CBA. *J Natl Cancer Inst* 1950;**11**: 581-592.
- 8 12. Leighton PA, Saam JR, Ingram RS, Stewart CL, Tilghman SM. An enhancer deletion
9 affects both H19 and Igf2 expression. *Genes Dev* 1995;**9**: 2079-2089.
- 10 13. Vernucci M, Cerrato F, Besnard N, Casola S, Pedone PV, Bruni CB, Riccio A. The H19
11 endodermal enhancer is required for Igf2 activation and tumor formation in experimental liver
12 carcinogenesis. *Oncogene* 2000;**19**: 6376-6385.
- 13 14. Lederer M, Bley N, Schleifer C, Huttelmaier S. The role of the oncofetal IGF2
14 mRNA-binding protein 3 (IGF2BP3) in cancer. *Semin Cancer Biol* 2014;**29C**: 3-12.
- 15 15. Sell S, Becker FF, Leffert HL, Watabe L. Expression of an oncodevelopmental gene product
16 (alpha-fetoprotein) during fetal development and adult oncogenesis. *Cancer Res* 1976;**36**:
17 4239-4249.
- 18 16. Nordin M, Bergman D, Halje M, Engstrom W, Ward A. Epigenetic regulation of the
19 Igf2/H19 gene cluster. *Cell Prolif* 2014;**47**: 189-199.
- 20 17. Grozdanov PN, Yovchev MI, Dabeva MD. The oncofetal protein glypican-3 is a novel

- 1 marker of hepatic progenitor/oval cells. *Lab Invest* 2006;**86**: 1272-1284.
- 2 18. Finkielstain GP, Forcinito P, Lui JC, Barnes KM, Marino R, Makaroun S, Nguyen V,
3 Lazarus JE, Nilsson O, Baron J. An extensive genetic program occurring during postnatal growth in
4 multiple tissues. *Endocrinology* 2009;**150**: 1791-1800.
- 5 19. Okada H, Kimura MT, Tan D, Fujiwara K, Igarashi J, Makuuchi M, Hui AM, Tsurumaru M,
6 Nagase H. Frequent trefoil factor 3 (TFF3) overexpression and promoter hypomethylation in mouse
7 and human hepatocellular carcinomas. *Int J Oncol* 2005;**26**: 369-377.
- 8 20. Sun Q, Zhang Y, Liu F, Zhao X, Yang X. Identification of candidate biomarkers for
9 hepatocellular carcinoma through pre-cancerous expression analysis in an HBx transgenic mouse.
10 *Cancer Biol Ther* 2007;**6**: 1532-1538.
- 11 21. Hoffmann W. Trefoil factors TFF (trefoil factor family) peptide-triggered signals promoting
12 mucosal restitution. *Cell Mol Life Sci* 2005;**62**: 2932-2938.
- 13 22. Sohda T, Yun K, Iwata K, Soejima H, Okumura M. Increased expression of insulin-like
14 growth factor 2 in hepatocellular carcinoma is primarily regulated at the transcriptional level. *Lab*
15 *Invest* 1996;**75**: 307-311.
- 16 23. Sohda T, Iwata K, Soejima H, Kamimura S, Shijo H, Yun K. In situ detection of insulin-like
17 growth factor II (IGF2) and H19 gene expression in hepatocellular carcinoma. *J Hum Genet* 1998;**43**:
18 49-53.
- 19 24. Ariel I, Miao HQ, Ji XR, Schneider T, Roll D, de Groot N, Hochberg A, Ayes S. Imprinted
20 H19 oncofetal RNA is a candidate tumour marker for hepatocellular carcinoma. *Mol Pathol* 1998;**51**:

1 21-25.

2 25. Boyault S, Rickman DS, de Reynies A, Balabaud C, Rebouissou S, Jeannot E, Hérault A,
3 Saric J, Belghiti J, Franco D, Bioulac-Sage P, Laurent-Puig P, Zucman-Rossi J. Transcriptome
4 classification of HCC is related to gene alterations and to new therapeutic targets. *Hepatology*
5 2007;**45**: 42-52.

6 26. Yamamoto Y, Nishikawa Y, Tokairin T, Omori Y, Enomoto K. Increased expression of
7 H19 non-coding mRNA follows hepatocyte proliferation in the rat and mouse. *J Hepatol* 2004;**40**:
8 808-814.

9 27. Whittaker S, Marais R, Zhu AX. The role of signaling pathways in the development and
10 treatment of hepatocellular carcinoma. *Oncogene* 2010;**29**: 4989-5005.

11 28. Kato T, Miyamoto M, Date T, Yasui K, Taya C, Yonekawa H, Ohue C, Yagi S, Seki E,
12 Hirano T, Fujimoto J, Shirai T, Wakita T. Repeated hepatocyte injury promotes hepatic
13 tumorigenesis in hepatitis C virus transgenic mice. *Cancer Sci* 2003;**94**: 679-685.

14 29. Saenz Robles MT, Pipas JM. T antigen transgenic mouse models. *Semin Cancer Biol*
15 2009;**19**: 229-235.

16 30. Schirmacher P, Held WA, Yang D, Chisari FV, Rustum Y, Rogler CE. Reactivation of
17 insulin-like growth factor II during hepatocarcinogenesis in transgenic mice suggests a role in
18 malignant growth. *Cancer Res* 1992;**52**: 2549-2556.

19 31. Stegmaier P, Voss N, Meier T, Kel A, Wingender E, Borlak J. Advanced computational
20 biology methods identify molecular switches for malignancy in an EGF mouse model of liver cancer.

1 *PLoS One* 2011;**6**: e17738.

2 32. Niwa T, Ushijima T. Induction of epigenetic alterations by chronic inflammation and its
3 significance on carcinogenesis. *Adv Genet* 2010;**71**: 41-56.

4 33. Easwaran H, Tsai HC, Baylin SB. Cancer epigenetics: tumor heterogeneity, plasticity of
5 stem-like states, and drug resistance. *Mol Cell* 2014;**54**: 716-727.

6

Table 1. Top 10 highly-expressed genes in CCl₄-induced tumors in Cluster C

Gene	Fold change vs. control (log ₂)		
	Cirrhosis (CCl ₄ -NT)	CCl ₄ tumor (CCl ₄ -T)	DEN tumor (DEN-T)
Insulin-like growth factor 2 (<i>Igf2</i>)	6.97	9.70	3.06
Lymphocyte antigen 6 complex, locus D (<i>Ly6d</i>)	6.46	8.33	6.55
Carboxypeptidase E (<i>Cpe</i>)	3.77	8.21	7.68
H19 fetal liver mRNA (<i>H19</i>)	5.48	8.13	6.47
Secretory leukocyte peptidase inhibitor (<i>Sipi</i>)	3.52	6.92	6.35
Keratin 20 (<i>Krt20</i>)	4.70	6.83	4.41
Stearoyl-Coenzyme A desaturase 2 (<i>Scd2</i>)	4.86	6.51	5.65
Topoisomerase (DNA) II alpha (<i>Top2a</i>)	5.03	6.18	3.89
Calcium and integrin binding family member 3 (<i>Cib3</i>)	3.76	6.15	3.58
Carbonyl reductase 3 (<i>Cbr3</i>)	2.55	6.04	2.35

Table 2. Top 10 highly-expressed genes in DEN-induced tumors in Cluster D

Gene	Fold change vs. control (log2)		
	Cirrhosis (CCl ₄ -NT)	CCl ₄ tumor (CCl ₄ -T)	DEN tumor (DEN-T)
Glypican 3 (<i>Gpc3</i>)	2.63	6.06	8.62
Aldo-keto reductase family 1, member C18 (<i>Akr1c18</i>)	3.26	6.44	8.57
Flavin containing monooxygenase 3 (<i>Fmo3</i>)	0.60	1.90	7.33
ATP-binding cassette, sub-family D, member 2 (<i>Abcd2</i>)	3.89	4.90	7.32
Tetraspanin 8 (<i>Tspan8</i>)	3.92	6.29	7.23
Alpha fetoprotein (<i>Afp</i>)	4.19	4.47	7.11
Trefoil factor 3, intestinal (<i>Tff3</i>)	0.91	6.30	6.98
Serine peptidase inhibitor, Kazal type 3 (<i>Spink3</i>)	6.68	6.22	6.92
Patatin-like phospholipase domain containing 5 (<i>Pnpla5</i>)	1.94	3.88	6.53
Cyclin-dependent kinase inhibitor 2B (<i>Cdkn2b</i>)	1.84	4.73	5.96

1 **Figure Legends**

2

3 **Figure 1.** Identification of differentially expressed genes in mouse liver tumors induced in cirrhotic
4 and noncirrhotic models. **a:** The gross appearance of the livers from control (olive oil-treated,
5 32-week-old), CCl₄-treated (32-week-old), and DEN-treated mice (46-week-old). **b:** Histology of the
6 liver tissues from control, CCl₄-treated, and DEN-treated mice. HE and sirius red staining. NT:
7 non-tumor; T: tumor. The arrows indicate the boundary of a DEN-induced tumor. Scale bar = 50 μm.
8 **c:** cDNA microarray analysis showing genetic clusters (A-D) of differentially expressed genes in
9 control liver tissues (olive oil-treated), CCl₄-induced cirrhotic tissues (CCl₄-NT), CCl₄-induced
10 tumors (CCl₄-T), and DEN-induced tumors (DEN-T).

11

12 **Figure 2.** Differential expression of mRNA and their products in CCl₄-induced and DEN-induced
13 liver tumors. **a:** RT-qPCR analyses of mRNA expression of 15 tumor-associated genes. The genes
14 preferentially expressed in CCl₄-induced tumors and DEN-induced tumors are designated as
15 “CCl₄-associated” and “DEN-associated,” respectively, and the genes comparatively expressed in
16 CCl₄-induced and DEN-induced tumors are designated as “Common.” Each value is expressed as the
17 mean ± SEM. The ages of the mice at analyses were 32-34 weeks and 46 weeks in the CCl₄-induced
18 and DEN-induced models, respectively. The number of samples in each group was 5, 12, 15, 6, and
19 13 for CCl₄ control (olive oil, C), CCl₄-induced cirrhosis (NT), CCl₄-induced tumors (T), DEN

1 control (NT), and DEN-induced tumors (T), respectively. *P<0.05, **P<0.01, ***P<0.001;
2 compared with control; one-way factorial ANOVA. **b:** *In situ* detection of IGF2, *H19* mRNA, TFF3,
3 and AFP in CCl₄-induced and DEN-induced tumors. Immunohistochemistry for IGF2, TFF3, and
4 AFP and *in situ* hybridization for *H19* mRNA. NT: non-tumor; T: tumor. Scale bar = 20 μm.

5

6 **Figure 3.** The relationship between the mRNA expression of tumor-associated genes and tumor cell
7 proliferation. Scatter plots of mRNA expression levels of selected tumor-associated genes and Ki-67
8 labeling index (%) in CCl₄-induced tumors (n =16) and DEN-induced tumors (n = 15). Spearman
9 correlation coefficients were used to test the association of mRNA expression and tumor cell
10 proliferation.

11

12 **Figure 4.** Fetal/neonatal activation of tumor-associated genes and their products. **a:** RT-qPCR
13 analyses of mRNA expression of the tumor-associated genes during the fetal/neonatal periods. Each
14 value is expressed as the mean ± SEM. The number of samples in each group was 3, 5, 7, 10, 4, 4, 4,
15 and 7 for E13.5, E16.5, P0 (immediately after birth), P1 (1 day after birth), P3 (3 days after birth), P6
16 (6 days after birth), 1 m (one-month-old), and 5 m (5-month-old), respectively. *P<0.05, **P<0.01,
17 ***P<0.001; compared with control (5 m); one-way factorial ANOVA. **b:** *In situ* detection of IGF2,
18 *H19* mRNA, TFF3, and AFP in developing livers. Immunohistochemistry for IGF2, TFF3, and AFP
19 and *in situ* hybridization for *H19* mRNA in fetal (E16.5) and neonatal (P0) livers. Scale bar = 20 μm.

1
2
3
4
5
6
7
8
9
10
11

Figure 5. Differential gene expression in TAA-induced liver tumors and spontaneously developed liver tumors. **a:** Histology of the liver tissues from TAA-induced and spontaneous tumors. The ages of mice at analyses were 38-40 weeks and 13-15 months in the TAA-induced model and spontaneous model, respectively. HE staining. NT: non-tumor; T: tumor. Scale bar = 50 μ m. **b:** RT-qPCR analyses of mRNA expression of 15 tumor-associated genes in TAA-induced and spontaneous tumors. Each value is expressed as the mean \pm SEM. The number of samples in each group was 7, 6, 9, 4, and 3 for the TAA control (C), TAA-induced cirrhosis (NT), TAA-induced tumors (T), control C3H mouse liver (NT), and spontaneous tumors (T) in C3H mice, respectively. * $P < 0.05$, ** $P < 0.01$, *** $P < 0.001$; compared with control; one-way factorial ANOVA.

12 **Figure 6.** Heatmap of two-dimensional hierarchical clustering of mRNA expression of the 15
13 tumor-associated genes in the 4 different liver tumor models (CCl₄-induced, DEN-induced,
14 TAA-induced, and spontaneous).

15
16 **Figure 7.** Association between the mRNA expression of *Igf2* and its related genes in CCl₄- and
17 TAA-induced tumors. **a:** Scatter plot showing a positive correlation between the mRNA expression
18 of *Igf2* and *H19* in CCl₄-induced tumors (n = 27) and TAA-induced tumors (n = 9). Spearman
19 correlation coefficient was used to test the correlation between the expression of the transcripts. **b:**

1 *Igf2bp3* mRNA expression in tumors with substantial *Igf2* mRNA expression ($Igf2^{high}$: $Igf2/Gapdh \geq$
2 0.01; CCl₄-induced tumors: n = 12; TAA-induced tumors: n = 3) and very low or no *Igf2* mRNA
3 expression ($Igf2^{low}$: $Igf2/Gapdh < 0.01$; CCl₄-induced tumors: n = 19; TAA-induced tumors: n = 6).
4 **P<0.01; unpaired two-tailed *t*-test.

5

6 **Figure 8.** Expression of IGF2, TFF3, and AFP in human HCC with or without liver fibrosis. **a:**
7 Immunohistochemistry for IGF2, TFF3, and AFP in human HCC and the surrounding cirrhotic
8 tissues. Scale bar = 20 μ m. **b:** Expression of IGF2, TFF3, and AFP in HCC developed in
9 noncirrhotic and cirrhotic livers. Tumors containing clusters of cells with unequivocal cytoplasmic
10 staining were regarded as positive (+).

Fig. 1 (Chen et al.)

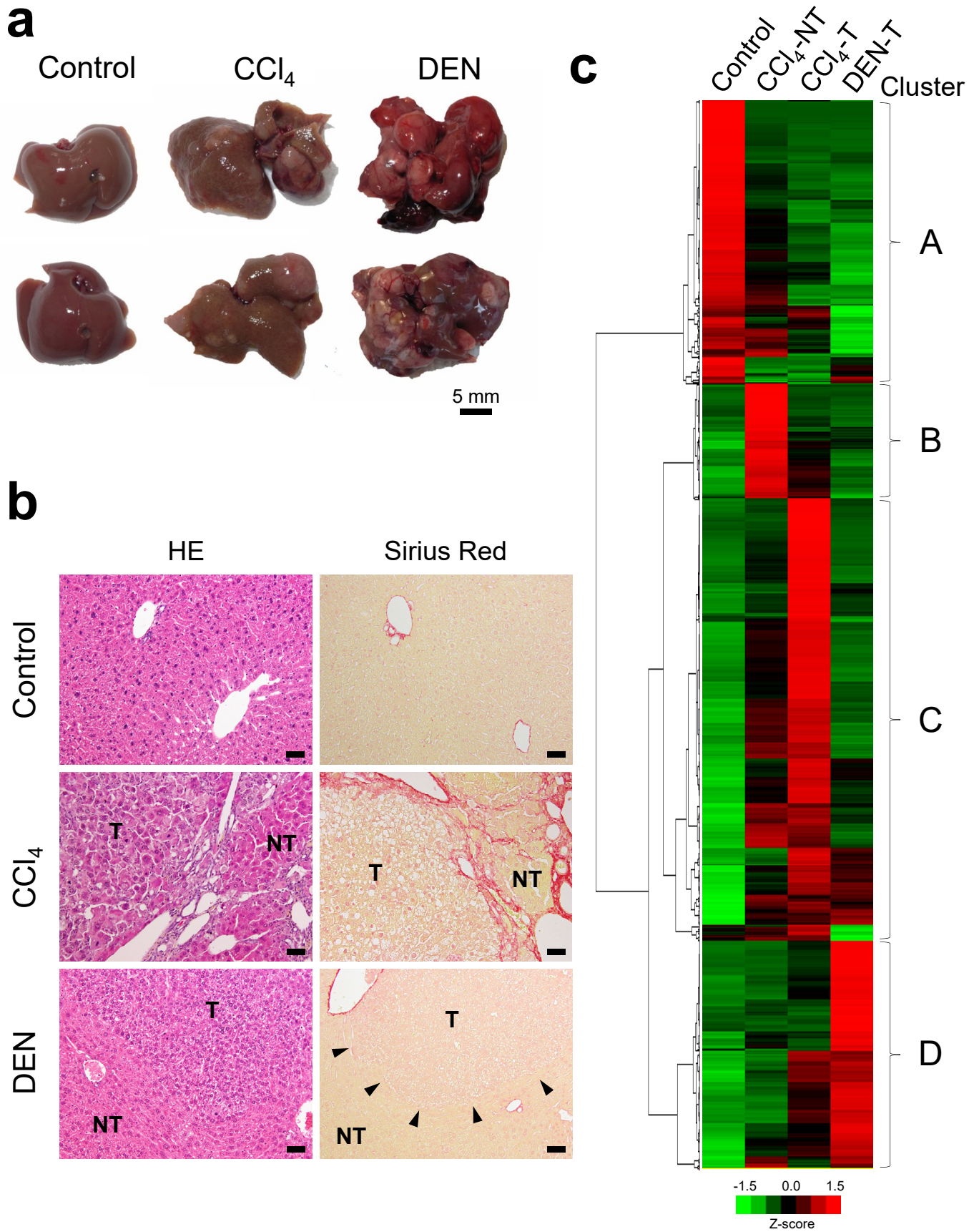


Fig. 2 (Chen et al.)

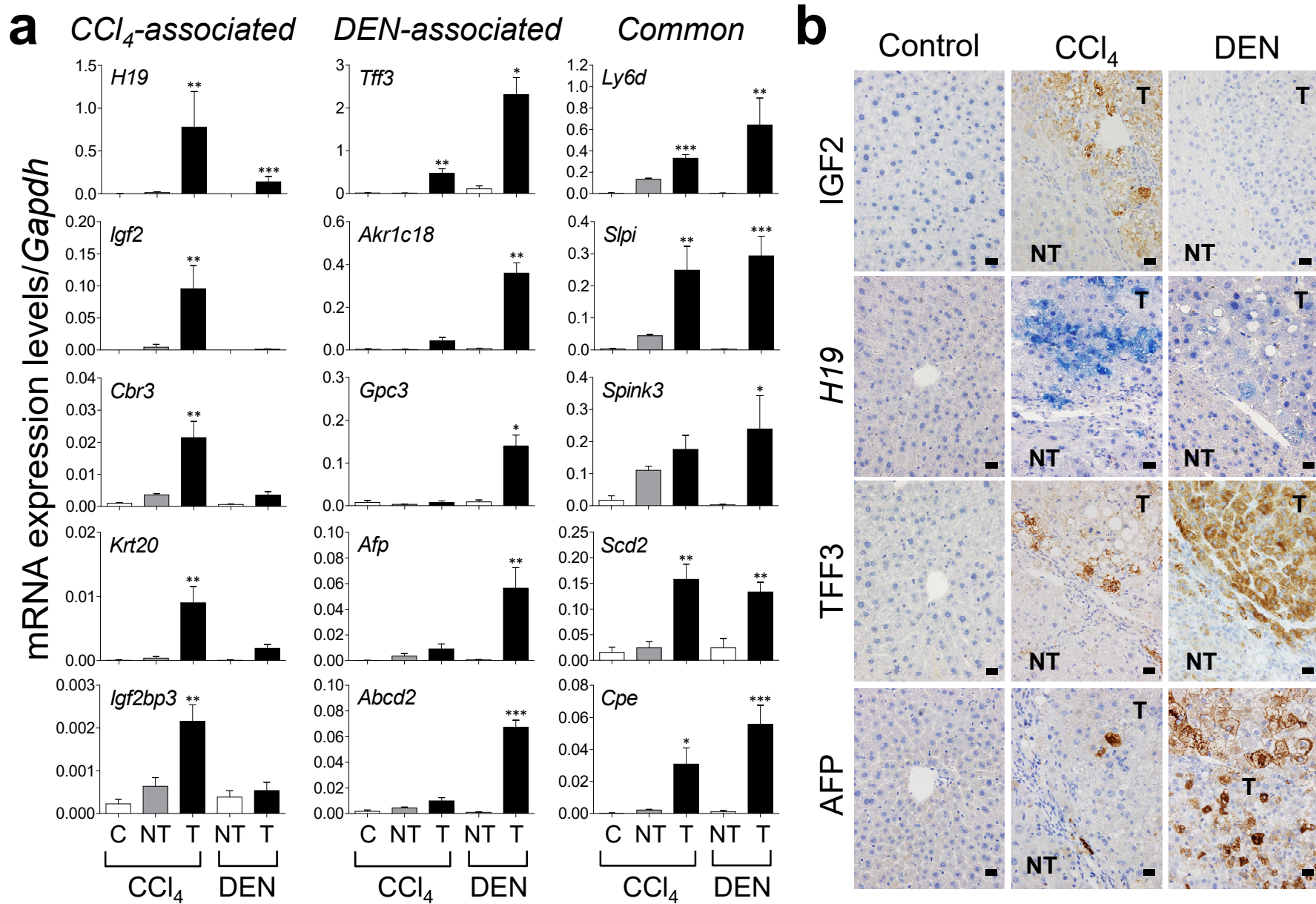
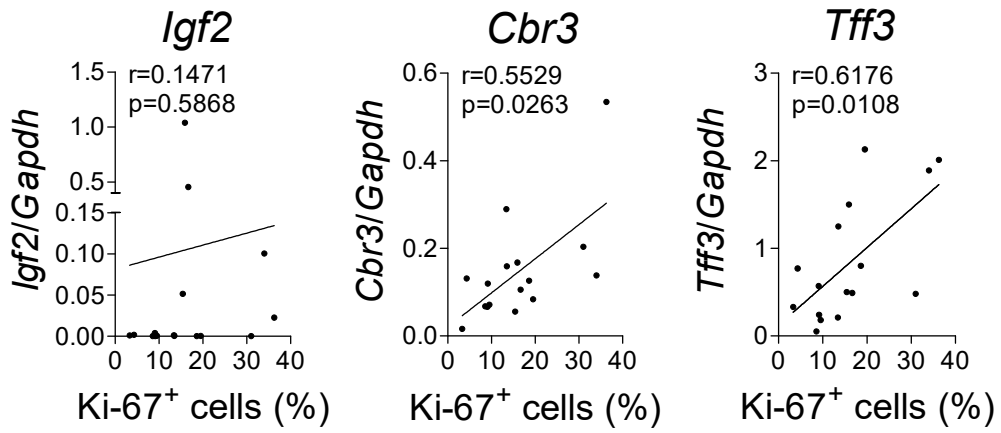


Fig. 3 (Chen et al.)

CCl₄-induced tumors



DEN-induced tumors

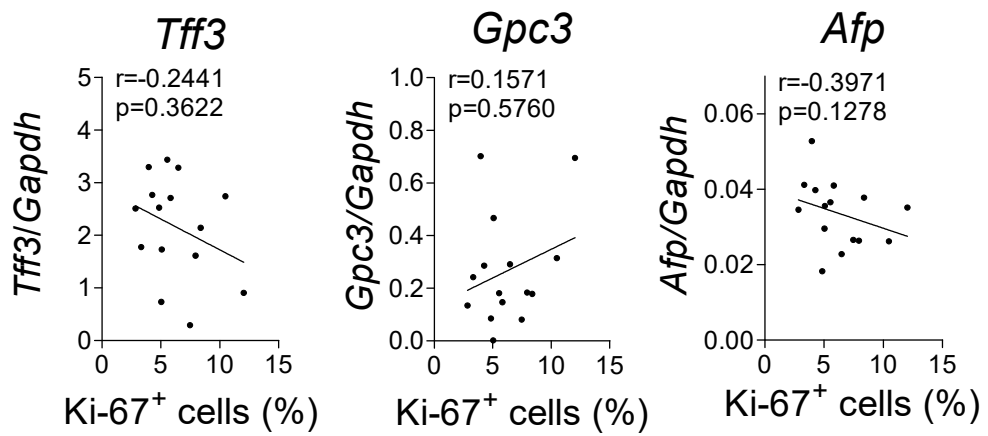


Fig. 4 (Chen et al.)

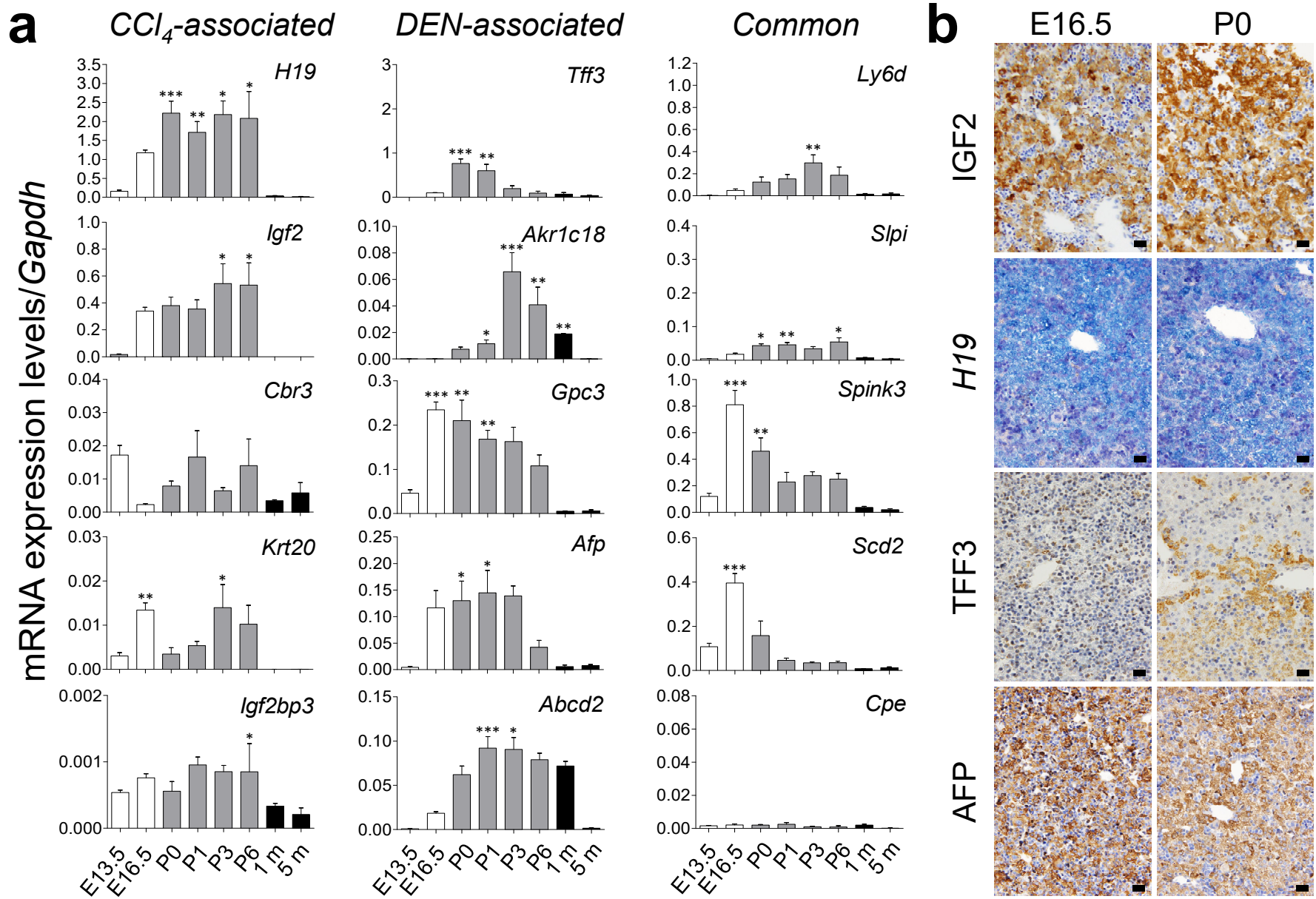


Fig. 5 (Chen et al.)

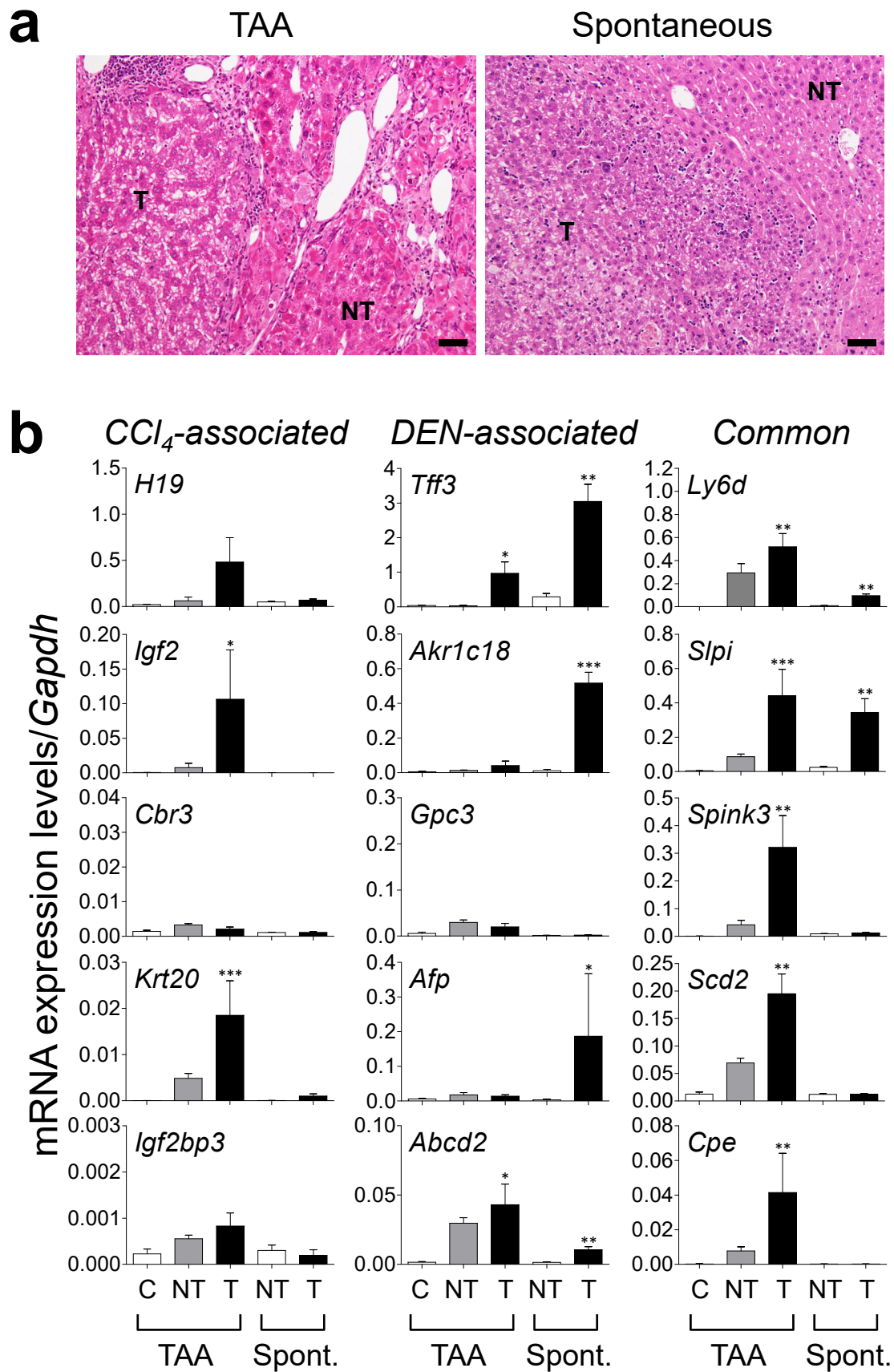


Fig. 6 (Chen et al.)

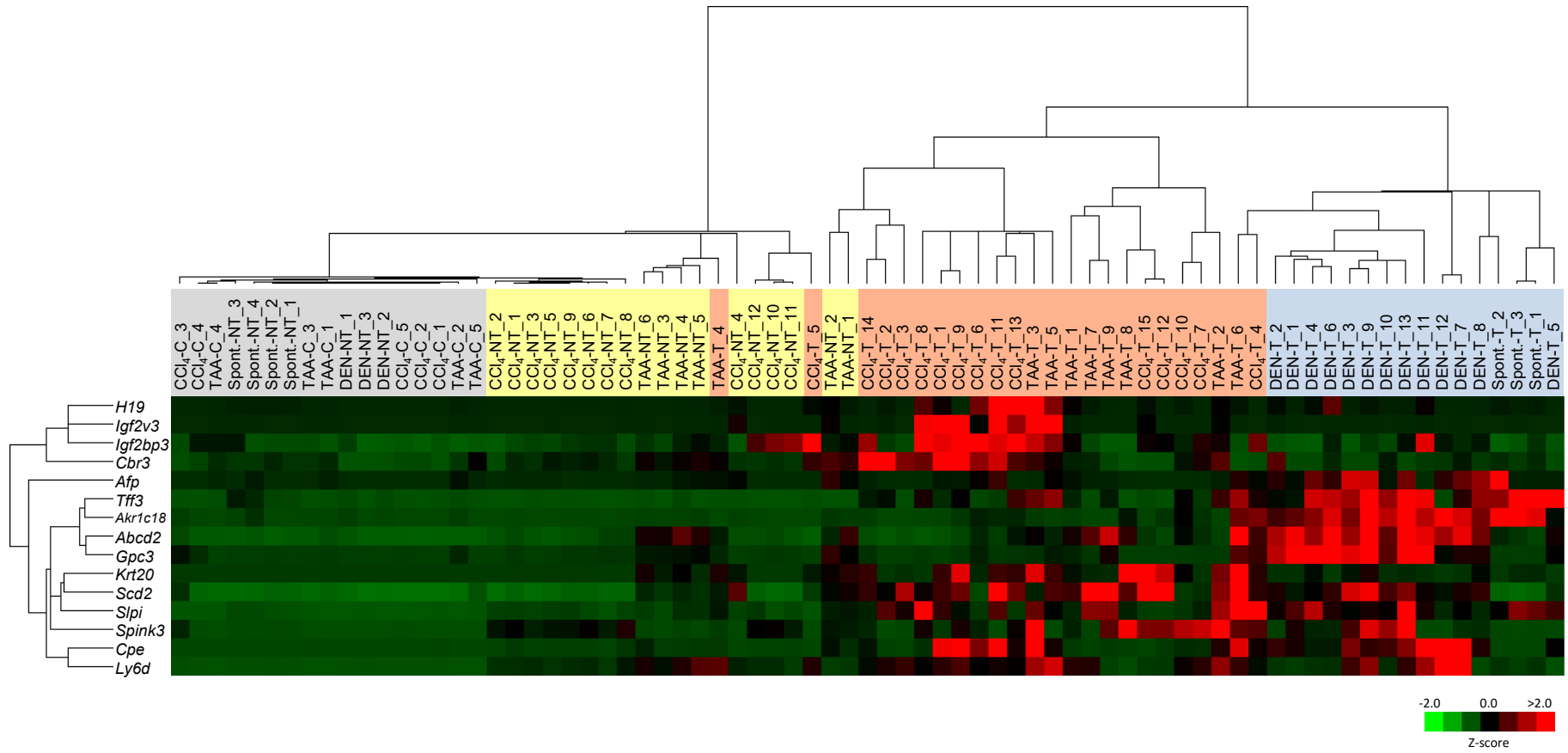
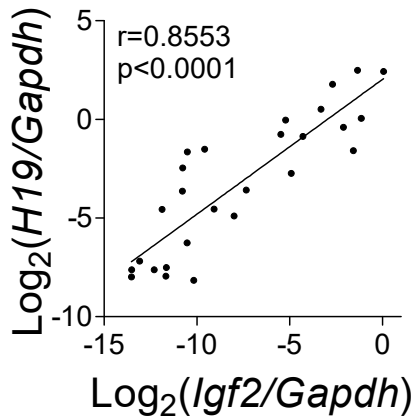


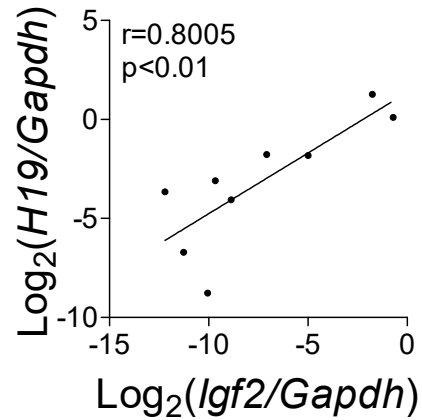
Fig. 7 (Chen et al.)

a

CCl₄-induced tumors

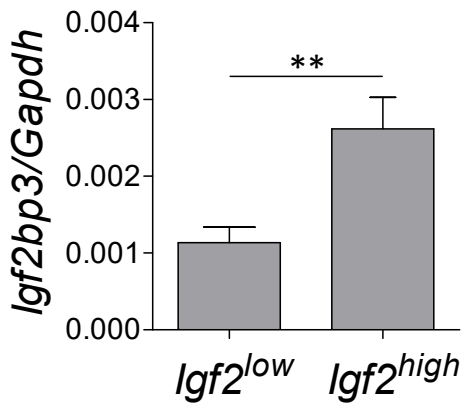


TAA-induced tumors



b

CCl₄-induced tumors



TAA-induced tumors

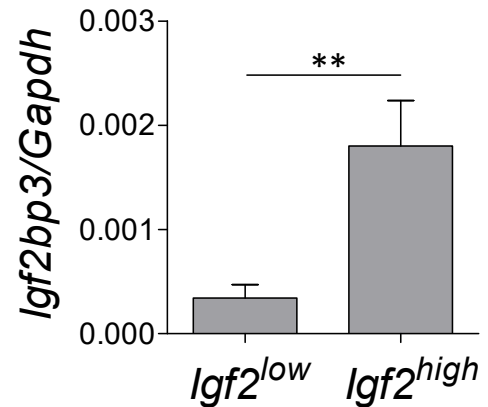
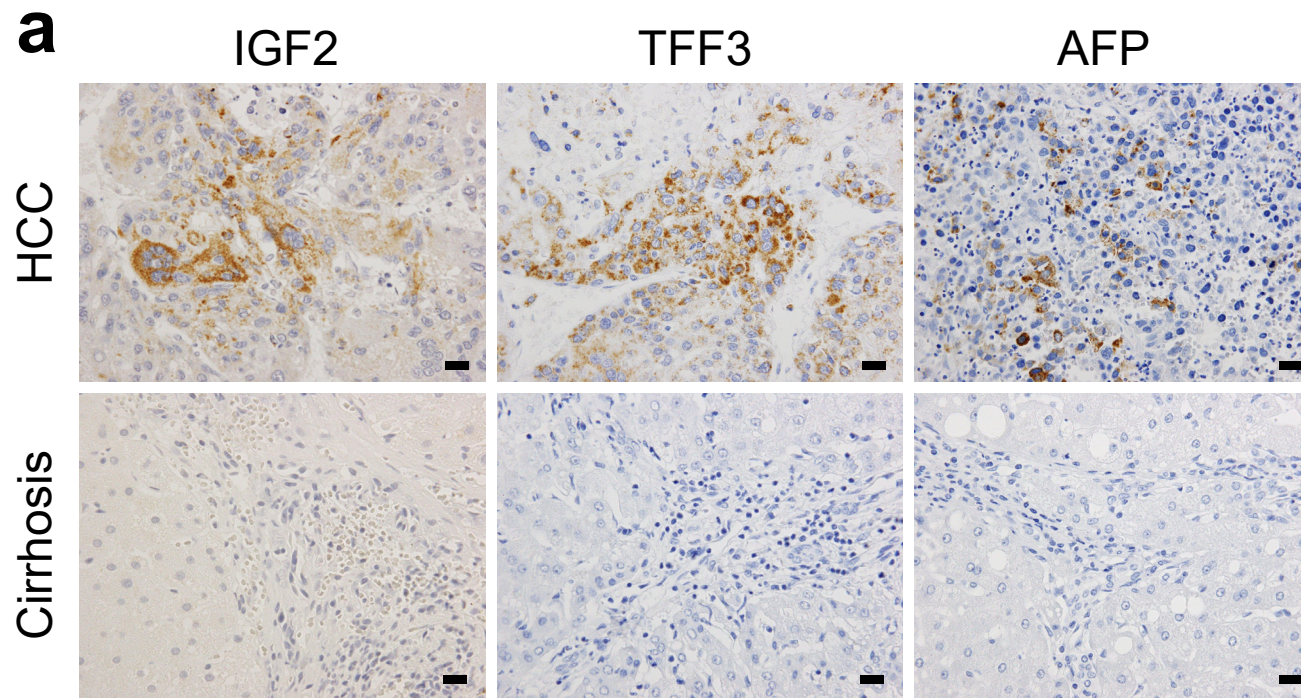


Fig. 8 (Chen et al.)



b

	Surrounding liver tissues				P-value (Fisher's exact test)
	Nonfibrotic (n = 9)		Fibrotic (n = 24)		
	+	-	+	-	
IGF2	1 (11.1%)	8 (88.9%)	13 (54.2%)	11 (45.8%)	0.0466
TFF3	4 (44.4%)	5 (55.6%)	7 (29.2%)	17 (70.8%)	0.1460
AFP	3 (33.3%)	6 (66.7%)	6 (25.0%)	18 (75%)	0.2753

Table S1. Primer sequences

Gene	Forward (5'->3')	Reverse (5'->3')
Insulin-like growth factor 2 variant 3 (<i>IGF2v3</i>)	CCTCCTTACCCAACCTTCAGGT	AAGAGATGAGAAGCACCAACATC
Lymphocyte antigen 6 complex, locus D (<i>Ly6d</i>)	TGCCCGTCCAACCTTCTACTTCT	TAGTCGGAGGTGCATGAGTTTG
Carboxypeptidase E (<i>Cpe</i>)	CTCATCAGCTACCTGGAGCA	AGCAAGCAATCGCCAGTAAT
H19, imprinted maternally expressed transcript (<i>H19</i>)	GTGTCACCAGAAGGGGAGTG	AGTGCCTCATGGGAATGGTG
Secretory leukocyte peptidase inhibitor (<i>Slpi</i>)	GCTGTGAGGGTATATGTGGGAAA	CGCCAATGTCAGGGATCAG
Keratin 20 (<i>Krt20</i>)	GCCCAGTGCGTCCTGCGAAT	GGCCTGGAGCAGCATCCACC
Stearoyl-coenzyme A desaturase 2 (<i>Scd2</i>)	GTTTGAAAGCTTTGGGTAGGG	AAGGCCCTAAAGCCTCTCTCT
Topoisomerase (DNA) II alpha (<i>Top2a</i>)	CACAATTGGCCATCTCTTCTGCGAC	TTCCTTAGCTTCCTTTGATGTGC
Calcium and integrin binding family member 3 (<i>Cib3</i>)	AGAGGCAGGTCTGGATCA	CTTGGGACTGGTCGTGTAGT
Carbonyl reductase 3 (<i>Cbr3</i>)	GTAAGTGGGGCTAACAAAGGC	TTGACCAGCACGTTAAGTCCC
Clypican 3 (<i>Gpc3</i>)	CCAGGTTTCCAAGTCACTG	CTTGAGGTGGTCGGTAGTGT
Aldo-keto reductase family 1, member C18 (<i>Akr1c18</i>)	GCACCATAGGCAACCAGAAC	TCTCATTCAATTTCCAGTGTCTC
Flavin containing monooxygenase 3 (<i>Fmo3</i>)	ACAAAGAAAAGGCACCCATG	CTCTCAAAGCATGTGGGCTC
ATP-binding cassette, sub-family D, member 2 (<i>Abcd2</i>)	CACAGCGTGACCTCTAC	AGGACATCTTTCCAGTCCA
Tetraspanin 8 (<i>Tspan8</i>)	ACCTAATGCCTTAGCAGCCATA	GCAAAGAAGTAGACAGAAGGAACAG
Alpha fetoprotein (<i>Afp</i>)	TGAAATTTGTCATGAGACGG	TGTCGTAAGTACTGAGCAGCCAAG
Trefoil factor 3 (<i>Tff3</i>)	CCCTCTGGCTAATGCTGTTG	GTGCATTCTGTCTCCTGCAG
Serine peptidase inhibitor, Kazal type 3 (<i>Spink3</i>)	CATGATGCAGTGGCGGGATG	CAGCAAGGCCACCTTTTTCG
Patatin-like phospholipase domain containing 5 (<i>Pnpla5</i>)	ACTGCCTTCAATGCCAGTTT	GCACTGGCTCCTTGTAAGT
Cyclin-dependent kinase inhibitor 2B (<i>Cdkn2b</i>)	CCAATCCAGGTCATGATGAT	CGTGCACAGGTCTGGTAAG
Glyceraldehyde 3-phosphate dehydrogenase (<i>Gapdh</i>)	TGTCCGTCGTGGATCTGAC	CCTGCTTCACCACCTTCTTG

Table S2. Top 10 highly-expressed genes in CCl₄-induced cirrhosis in Cluster B

Gene	Fold change vs. control (log2)		
	Cirrhosis (CCl ₄ -NT)	CCl ₄ tumor (CCl ₄ -T)	DEN tumor (DEN-T)
S100 calcium binding protein G (<i>S100g</i>)	9.14	3.64	3.46
Prostaglandin D2 synthase (brain) (<i>Ptgds</i>)	6.63	1.51	-0.66
Fatty acid binding protein 6, ileal (gastrotropin) (<i>Fabp6</i>)	5.56	4.59	-0.40
Cytochrome P450, family 4, subfamily a, polypeptide 14 (<i>Cyp4a14</i>)	5.09	-0.72	-2.05
Nuclear protein transcription regulator 1 (<i>Nupr1</i>)	5.02	1.75	1.82
Plasminogen activator, tissue (<i>Plat</i>)	4.70	5.21	2.23
Fibroblast growth factor 21 (<i>Fgf21</i>)	4.70	4.13	3.85
Matrix metalloproteinase 7 (<i>Mmp7</i>)	4.58	1.44	0.71
Very low density lipoprotein (<i>Vldlr</i>)	4.42	1.24	2.05
FXD domain-containing ion transport regulator 3 (<i>Fxyd3</i>)	4.37	0.78	1.03

1 **Supporting Figure Legends**

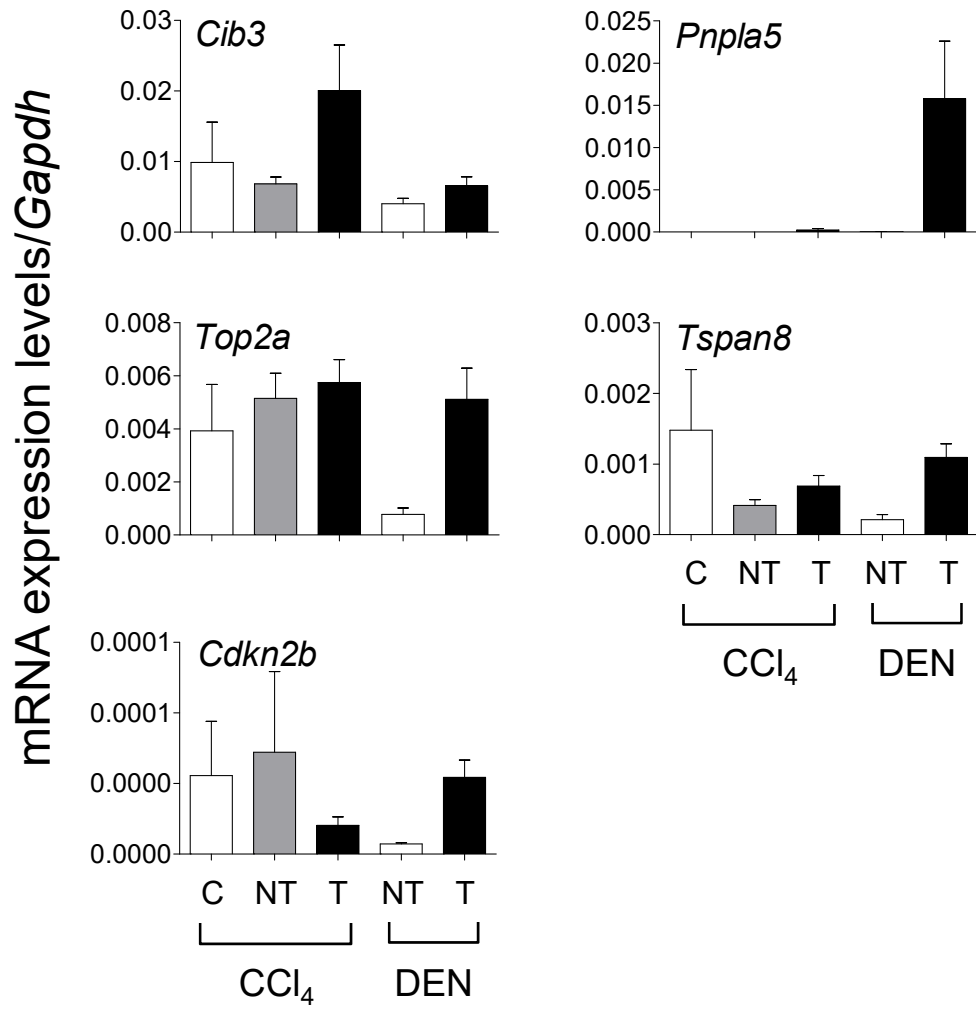
2

3 **Fig. S1.** RT-qPCR analyses of mRNA expression of Cib3, Top2a, Cdkn2b, Pnpla5, and Tspan8 in
4 CCl₄-induced and DEN-induced liver tumors. Each value is expressed as the mean \pm SEM. The
5 numbers of samples in each group was 5, 12, 15, 6, and 13 for the CCl₄ control (olive oil),
6 CCl₄-induced cirrhosis, CCl₄-induced tumors, DEN control, and DEN-induced tumors, respectively.

7

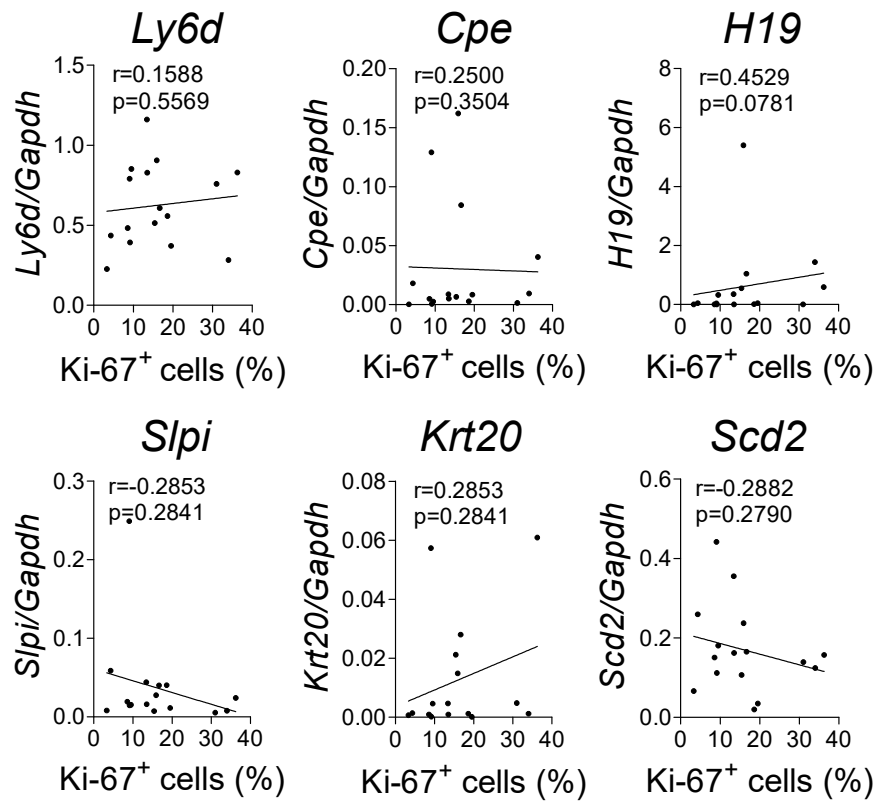
8 **Fig. S2.** The relationship between the mRNA expression of tumor-associated genes and tumor cell
9 proliferation. Scatter plots of mRNA expression levels of the tumor-associated genes by RT-qPCR
10 and Ki-67 labeling index (%) in CCl₄-induced tumors (n =16) and DEN-induced tumors (n = 15).
11 The data of the genes that were not included in Figure 4 are shown here. Spearman correlation
12 coefficients were used to test the association between mRNA expression and tumor cell proliferation.

Supporting Fig. 1 (Chen et al.)



Supporting Fig. 2 (Chen et al.)

CCl₄-induced tumors



DEN-induced tumors

